We are IntechOpen,
the world's leading publisher of
Open Access books
Built by scientists, for scientists

6,900
Open access books available

185,000
International authors and editors

200M
Downloads

154
Countries delivered to

Our authors are among the

TOP 1%
most cited scientists

12.2%
Contributors from top 500 universities

CLARIVATE ANALYTICS
BOOK CITATION INDEX
INDEXED

WEB OF SCIENCE™

Selection of our books indexed in the Book Citation Index
in Web of Science™ Core Collection (BKCI)

Interested in publishing with us?
Contact book.department@intechopen.com

Numbers displayed above are based on latest data collected.
For more information visit www.intechopen.com

Woven Fabrics Surface Quantification

Jiří Militký

Faculty of Textile Engineering, Technical University of Liberec, LIBEREC,
Czech Republic

1. Introduction

It was revealed (Kawabata, 1980) that surface roughness is one of the main characteristics of fabric responsible for hand feeling. On the other hand it was found (Militký & Bajzík, 2000) that paired correlation between subjective hand ratings and surface roughness is statistically not significant. Anisotropy of mechanical and geometrical properties of textile fabrics is caused by the pattern and non-isotropic arrangement of fibrous mass. Fabric structural pattern characteristics are important from point of view of fabric appearance uniformity and have huge influence on the surface roughness, which is an important part of mechanical comfort (Militký & Bajzík, 2001). The complex structural pattern depends on the appearance of warp and weft on their surface, very often, one group of threads dominates. Typical examples of patterned fabric are cords where the so called "rows" parallel with machine direction are created. In the so called non-patterned fabrics the surface appearance or roughness is usually dependent on the weave and uniformity of fabric creation (Militký & Bleša, 2008). From a general point of view, the fabrics rough surface displays two basic geometrical features:

1. Random aspect: the rough surface can vary considerably in space in a random manner, and subsequently there is no spatial function being able to describe the geometrical form,
2. Structural aspect: the variances of roughness are not completely independent with respect to their spatial positions, but their correlation depends on the distance. Especially surface of woven fabrics is characterized by nearly repeating patterns and therefore some periodicities are often identified.

Periodic fluctuations of surface roughness can be spatially dependent due to arrangements of weft and warp yarns. Non-periodic type of spatial dependence is subtler.

The main aims of this chapter are:

*   Characterization of fabrics surface profile i.e. "surface height variation (SHV) trace" by using of techniques based on the standard roughness evaluation, spatial analysis, Fourier regression, power spectral density (PSD) and utilization of fractal dimensions.
*   Indication of micro and macro roughness by using of aggregation principle or by using of selected frequencies in PSD.
*   The characterization of roughness anisotropy by using of profile spectral moments.

- Description of approach for contact-less evaluation of surface relief (macro roughness). This approach is based on the image analysis of especially prepared fabric images.

The simulated "teeth" profiles with variable height and thickness is used for identification of all kind of roughness parameters capability. These parameters are applied for characterization of some real patterned and non-patterned fabrics surface roughness.

2. Measurement of surface profiles

Surface irregularity of planar textiles can be identified by contact and contact-less techniques. For **contact measurements** the height variation (as thickness meter) or measurement of force needed for tracking the blade on the textile surface is applied (Ajayi, 1992, 1994; Militký & Bajzík, 2001, 2004). **Contacts less measurements** are usually based on the image analysis of fabric surfaces (Militký & Bleša, 2008). The subjective assessment of the fabrics roughness can be investigated as well (Stockbridge H.C. et. al, 1957).

KES for hand evaluation (Kawabata 1980) contains measuring device for registration the surface height variation (SHV) trace. This device (shown in the fig. 1) is a part of system KES produced by company KATO Tech.

Fig. 1. Device for measurement of fabric surface characteristics

The main part of this device is contactor (see. fig. 2) in the form of wire having diameter 0.5 mm. The contact force 10 g is used.

Fig. 2. KES contactor for measuring of surface roughness

This contactor touches on the sample under the standardized conditions. The up and down displacement of this contactor caused by surface roughness is transduced to the electric

signal by a linear transformer put at up ends of the contactor. The signal from the transducer is passed to the high pass digital filter having prescribed frequency response (wavelength being smaller than 1 mm). The sample is moved between 2 cm interval by a constant rate 0.1 cm/sec on a horizontal smooth steel plate with tension 20g/cm and SHV is registered on paper sheet. The SHV corresponds to the surface profile in selected direction (usually in the weft and warp directions are used for SHV creation).

The preprocessing of SHV traces, from images of paper sheet resulting form KES can be divided into the two phases.

- Digitalization of trace picture by image analysis system
- Removing parasite objects (grid, axes, base line etc.)

First of all the low ω_L and high ω_H surface frequency bands have to be specified. These cut-off frequencies are related to the wavelength limits l_L and l_H i.e. $l_L = 2\pi / \omega_L$ and $l_H = 2\pi / \omega_H$. The low pass cut-off is related to Nyquist criterion i.e. $l_L = dp / 2$ and the high pass cut-off is dependent on the maximum intersecting wavelength. For non-regular SHV, $l_H = L$ has to be selected. The results of digitalization and parasite object removing is set of "clean" heights $R(d_i)$ of fabric in places $0 < d < L$ (L is maximum investigated sample length and $i = 1 \ldots M$ is number of places). The distance between places $d_p = d_{i+1} - d_i$ is constant. For the case of Kawabata device L = 2 cm and $d_p = 2/(N-1)$ cm.

For deeper evaluation of SHV from KES device the rough signal from transducer has been registered and digitalized by using of LABVIEW system (Militký, 2007). Result is output voltage $U(d)$ in various distances d from origin of measurements. For calibration of this signal the mean value $E(U)$ and variances $D(U)$ were estimated. From KES apparatus the mean thickness $\bar{R}$ and corresponding standard deviation S_R were obtained. The transformation form voltage $U(d)$ to thickness $R(d)$ was realized by means of relation

$$R(d) = \bar{R} + S_R \left(\frac{U(d) - E(d)}{\sqrt{D(d)}} \right) \tag{1}$$

The result of this treatment is raw thickness $R(d)$ in various distances d from origin.

The technique of roughness evaluation will be demonstrated on the analysis of the surface trace SHV of twill fabric (see fig 3) in the machine direction.
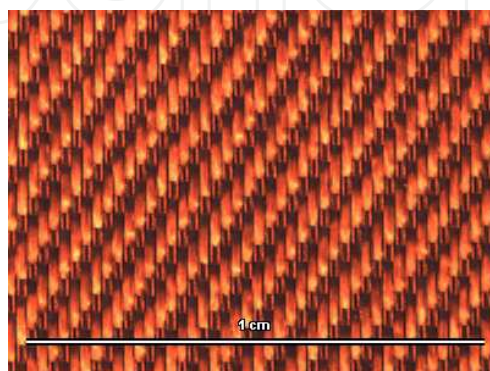

Fig. 3. Twill fabric used for roughness evaluation

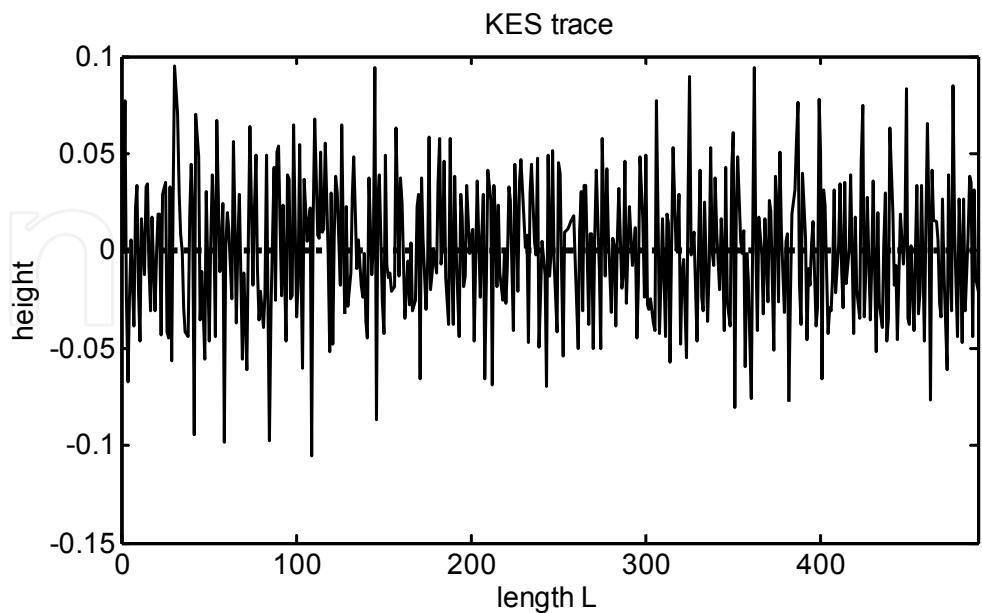The raw SHV trace of twill fabric is shown in the fig. 4.

Fig. 4. SHV trace from LABVIEW

Similar approach is based on the measurement of R(d) by Shirley step thickness meter with replacement of measuring head by blade (Militký & Bajzík, 2001). The Shirley step thickness meter is shown in the fig. 5.

Fig. 5. The step thickness meter SDL M 034/1

The principle of profile roughness evaluation by the simple accessory to the tensile testing machine is registration of the force *F(d)* needed for tracking the blade on the textile surface (Militký & Bajzík, 2004). Roughly speaking, the *F(d)* should be proportional to the *R(d)*. In reality, the *F(d)* profile is different due to small surface deformation caused by the tracked blade. Based on the complex testing the following working conditions have been selected:

Blade contact pressure 0.2 mN

Blade movement rate 0.6 mm/s
Sampling frequency 50 s^{-1} (length between samples Δd = 0.013 mm)
Investigated length T = 30 mm

The arrangement of this accessory to the tensile testing machine is shown in fig. 6.
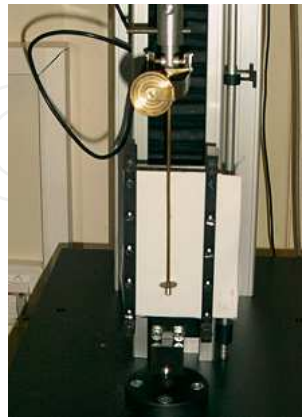

Fig. 6. Accessory for roughness evaluation by the tensile testing machine

Output from measurements is sequence of loads $F(d_i)$.

Variation of thickness $R(d_i)$ or loads $F(d_i)$ can be generally assumed as combination of random fluctuations (uneven threads, spacing between yarns, non uniformity of production etc.) and periodic fluctuations caused by the repeated patterns (twill, cord, rib etc.) created by weft and warp yarns. For description of roughness the characteristics computed from $R(d)$ or $F(d)$ in places $0< d< T$ (T is maximum investigated sample length and M is number of places) are used.

Profile of textile surfaces at given position along machine direction can be obtained by the analysis of especially prepared fabric images. The system RCM (Militký & Mazal, 2007) is composed from CCD camera, lighting system and special sample holder controlled by a personal computer (Fig. 7).
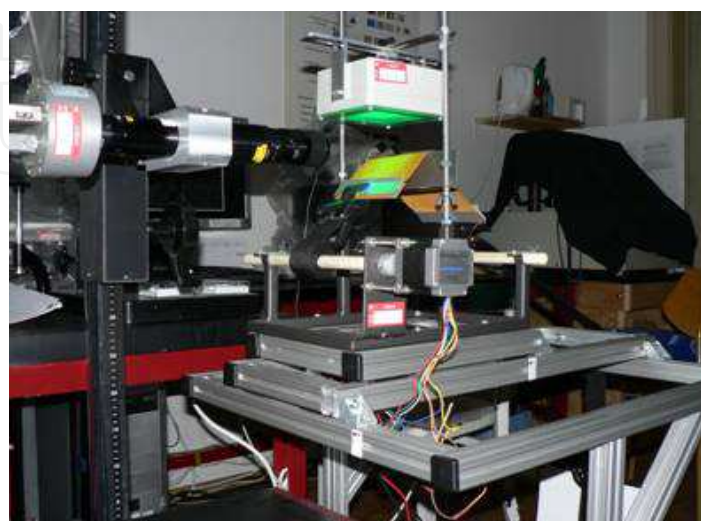

Fig. 7. Details of RCM apparatus

For good image creation the suitable lighting (laser from the top) and fabric arrangement (bend around sharp edge) were selected (see fig. 8).
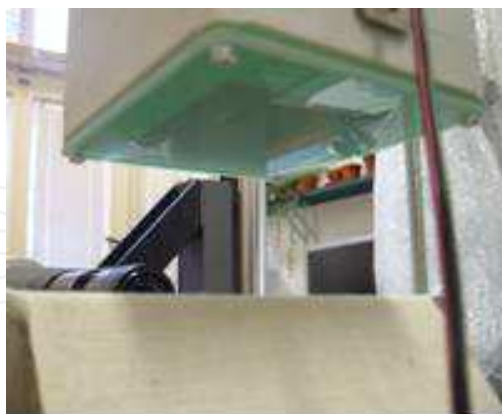

Fig. 8. Details of lighting system

Result after image treatment is so called "slice" which is the roughness profile in the cross direction at selected position in machine direction (the line transect of the fabric surface). The system RCM offers reconstruction of surface roughness plane in two dimensions. For this purpose, the sample holder is step by step moved in controlled manner. From set of these profiles, it is possible to reconstruct the surface roughness plane (Militký & Mazal, 2007).

A finished cord fabric with relatively good structural relief was selected for demonstration of relief creation system capability. The original fabric surface is shown in the fig. 9.
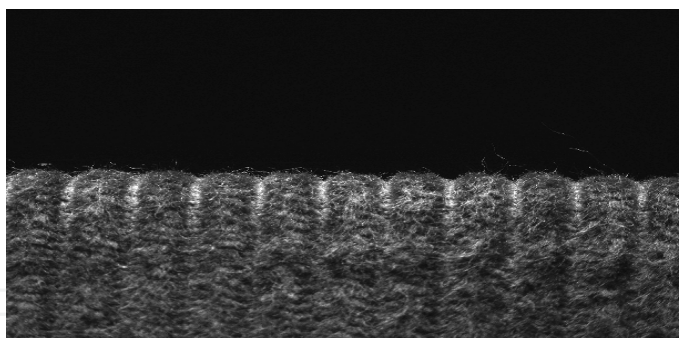

Fig. 9. Roughness profile in the cross direction of tested fabric

Individual relief slices were created by combination of threshold, set of morphological operations (erosion, dilatation) and Fourier smoothing to the 30 terms (Quinn & Hannan, 2001). Result of these operations is vector of surface heights in cross direction at specified machine direction (see fig. 10).

Fig. 10. Slice after morphological operations and cleaning

Output of data pre-treatment phase is array of slices i.e. array of vectors $R_{j(i)}$ where index i corresponds to the position in jth slice. From this array it is simple to reconstruct whole surface relief (see. fig. 11).
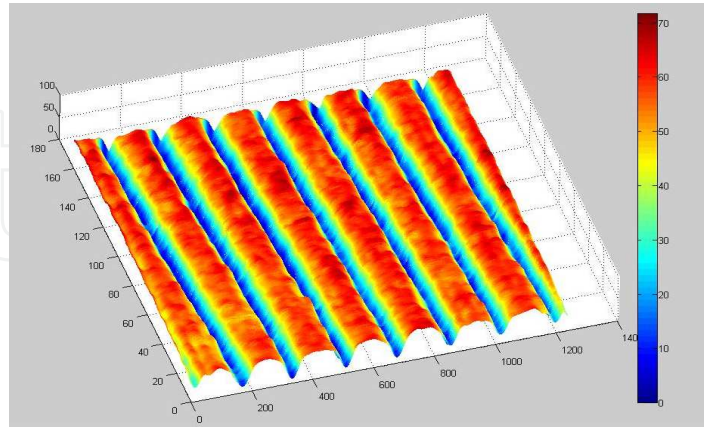

Fig. 11. Reconstructed roughness surface

Above described devices are based on the measurements of surface height variation (SHV) or force needed for tracking blade across of surface in given direction. The analysis of surface images in two dimensions is based on the different principles (Militký & Klička, 2007). These methods are not discussed in this chapter.

3. Surface roughness

There exists a vast number of empirical profile or surface roughness characteristics suitable often in very special situations (Quinn & Hannan, 2001; Zhang & Gopalakrishnan, 1996). Some of them are closely connected with characteristics computed from fractal models as fractal dimension and topothesy (Davies, 1999). A set of parameters for profile and surface characterization are collected in (Militký & Bajzík, 2003, Militký & Mazal, 2007). Parameters for profile and surface characterization can be generally divided into the following groups:

- Statistical characteristics of surface profile distribution (variance, skewness, kurtosis)
- Spatial characteristics as autocorrelation or variogram (denoted in engineering as structural function). Analysis is here in fact based on the analysis of random field moment characteristics of second order.
- Spectral characteristics as power spectral density or Fourier analysis.
- Characteristics of overall complexity based on random linear stationary processes, self-affined processes, long-range dependencies and on the theory of chaotic dynamics or nonlinear time series.

General surface topography is usually broken down to the three components according to wavelength (or frequency). The long wavelength (low frequency) range variation is denoted as form. This form component is removed by using of polynomial models or models based on the form shape. The low wavelength (high frequency) range variation is denoted as roughness and medium wavelength range variation separates waviness. The most common way to separate roughness and waviness is spectral analysis. This analysis is based on the Fourier transformation from space domain d to the frequency domain $\omega = 2\pi / d$.

Data from contact based measurements of roughness often represents height variation on line transects of the surface. Usually, it is possible to obtain structural data for one direction of the fabric, whereas the results on the other direction do not give clear information about the respective structural patterns. Some contacts-less methods based on the image analysis are found to be capable for measuring fabric structural pattern in the whole plane.

Standard methods of surface profile evaluation are based on the relative variability characterized by the variation coefficient - analogy with evaluation of yarns mass unevenness or simply by the standard deviation. This approach is used in Shirley software for evaluation of results for step thickness meter.

Common parameters describing roughness of technical surfaces are given in the ISO 4287 standard (Anonym, 1997). For characterization of roughness of textiles surfaces the mean absolute deviation MAD (SMD as per Kawabata) is usually applied (Meloun & Militký, 2011). The descriptive statistical approach based on the assumptions of independence and normality leads to biased estimators, if the SHV has short or long-range correlation. There is therefore necessity to distinguish between standard white Gauss noise and more complex models. For description of short range correlation the models based on the autoregressive moving average are useful (Maisel, 1971). The long-range correlation is characterized by the fractal models (Beran, 1984; Whitehouse, 2001). The deterministic chaos type models are useful for revealing chaotic dynamics in deterministic processes where variation appears to be random but in fact predictable. For the selection among above mentioned models the power spectral density (PSD) curve evaluated from experimental SHV can be applied (Eke, 2000; Quinn & Hannan, 2001).

Especially the fractal models (Mandelbrot & Van Ness, 1968) are widely used for rough surface description. For these models the dependence of log (PSD) on the log (frequency) should be linear. Slope of this plot is proportional to fractal dimension and intercept to the so-called topothesy. White noise has dependence of log (PSD) on the log (frequency), nearly horizontal plateau for all frequencies (the ordinates of PSD are independent and exponentially distributed with common variance). More complicated rough surfaces can be modeled by the Markov type processes. For these models the dependence of log (PSD) on the log (frequency) has plateau at small frequencies, then bent down and are nearly linear at high frequencies (Sacerdotti et. al, 2000). A lot of recent works is based on the assumption that the stochastic process (Brownian motion) can describe fabrics surface variation (Sacerdotti et. al, 2000). It is clear that for the deeper analysis of rough surface, the more complex approach should be used.

4. Simulated "teeth" profiles

The surface of cord fabrics has typical "teeth" in the machine direction. For indication of the influence of geometry of teeth on the values of the roughness characteristics the simulated roughness profile in the cross direction was created. The standard pattern is composed from two parts (see. fig. 12).

The top height of one tooth is selected as 1. Bottom height of one tooth is equal to the value of ym. The tooth size is therefore 1 – ym. The length of distance between teeth is equal to am and tooth thickness is equal 1- am. Total length of standard pattern equal to the 1 and 100 individual values are generated, i.e. the standard pattern is characterized by 100 points with

constant increment. Teeth profile is then composed from 11 repetitions of standard pattern. The simulated teeth profiles were generated for the set of value $0.1 \leq am \leq 0.9$, $0.1 \leq ym \leq 0.9$ with increment 0.1. The tooth profile for the case am = ym = 0.1 is shown in the fig. 13a and for the case of am = ym = 0.9 is shown in the fig. 13b.
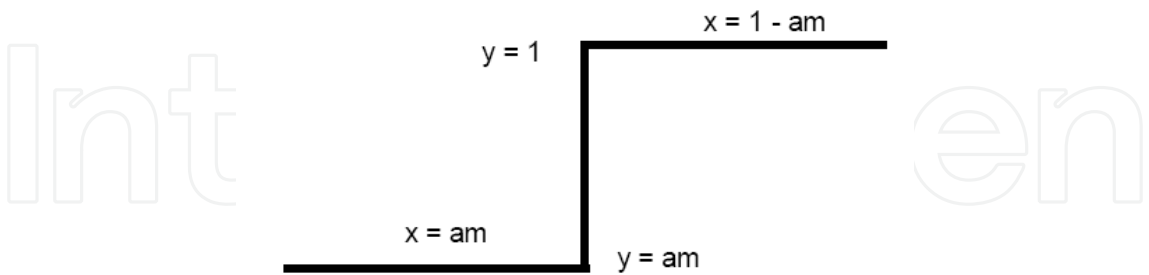

Fig. 12. Standard pattern

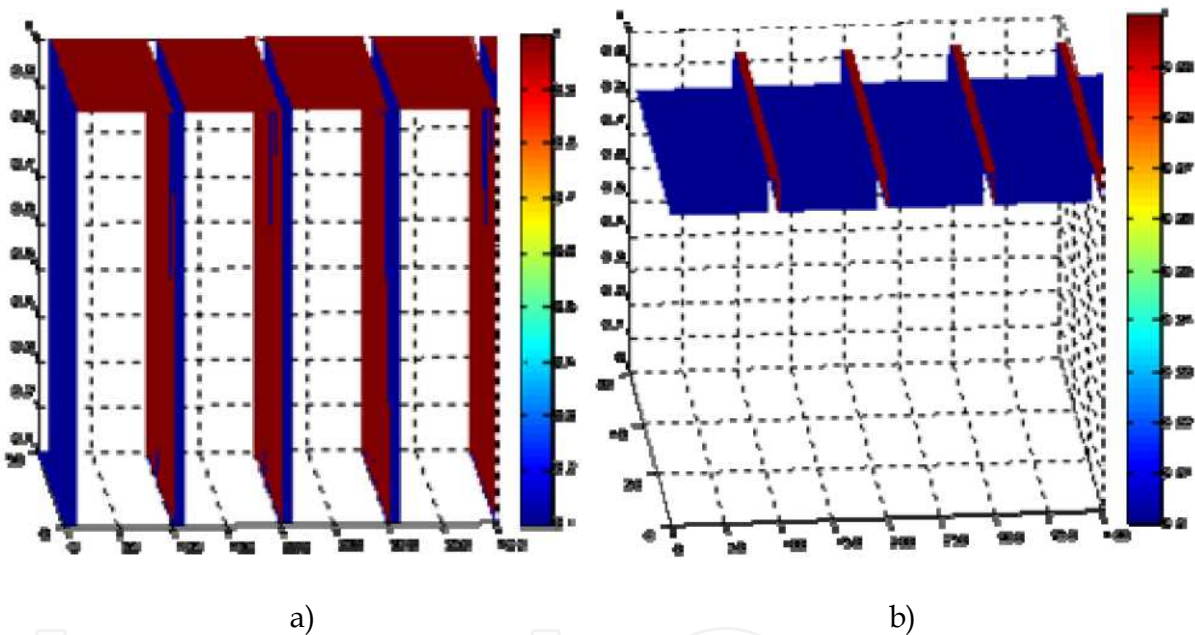a)   b)

Fig. 13. Detail of teeth profile for a) am = ym = 0.1 and for b)

It can be easily derived that the mean height R_a of teeth profile is equal to the

$$R_a = 1 - am(1 - ym) \tag{2}$$

Corresponding standard deviation SD is equal to

$$SD = \sqrt{\frac{1}{100}\left([100ym\,am]^2 + [100(1-ym)am]^2 - 100R_a{}^2\right)} \tag{3}$$

Some of the other characteristics can be analytically expressed as well but expressions are complicated. Generated teeth profiles were used for computation of profiles characteristics. The dependence of these characteristics on the am and ym are shown in subsequent paragraphs.

5. Basic assumptions testing

Consider a series $R_{(i)}$. Let this series is one "spatial" realization of random process $y = R(d)$. For analysis of this series it is necessary to know if some basic assumptions about behavior of underlying random process can be accepted or not. These basic assumptions are (Maisel, 1971):

- stationarity
- ergodicity
- independence

In fact the realizations of random process are $R_{j(i)}$, where index j correspond to individual realizations and index i corresponds to the distance d_i. In the case of ensemble samples there are values $R_{j(i)}$ for $i = const.$ and $j = 1. M$ at disposal.

For these data there is no problem to use standard statistical analysis of univariate samples for creation of data distribution e.g. probability density function $p(R_{(i)})$ or computation of statistical characteristics as mean value $E(R_{(i)})$ or variance $D(R_{(i)})$. In majority of applications, the ensemble samples are not available and statistical analysis is based on the one spatial realization $R_{j(i)}$ for j = 1 and i = 1.N. For creation of data distribution and computation of moments, some additional assumptions are necessary.

The basic assumption is stationarity. The random process is **strictly stationary** if all the statistical characteristics and distributions are independent on ensemble location. The **wide sense stationarity** of *g-th* order implies independence of first *g* moments on ensemble location.

The second order stationarity implies that:

- mean value $E(R_{(i)}) = E(R)$ is constant (not dependent on the location d_i).
- variance $D(R_{(i)}) = D(R)$ is constant (not dependent on the location d_i).
- autocovariance, autocorrelation and variogram, which are functions of d_i and d_j are not dependent on the locations but on the lag $h = |d_i - d_j|$ only.

For example the covariance is $c(R(d_i)\, R(d_{i+h})) = c(h)$. For ergodic process the "ensemble" mean can be replaced by the average across distance (from one spatial realization) and autocorrelation $R(h) = 0$ for all sufficiently high h.

Ergodicity is very important, as the statistical characteristics can be calculated from one single series $R_{(i)}$ instead of ensembles which frequently are difficult to be obtained. Given a $R_{(i)}$ series, the selection of the appropriate approach for its analysis is not a trivial task because the mathematical background of the underlying process is unknown. Moreover, the $R_{(i)}$ are corrupted by noise and consist of finite number of sample values. The task to analyze real data is often to resolve the so-called inverse problem, i.e., given a series $R_{(i)}$, how to discover the characteristics of the underlying process. Three approaches are mainly applied:

- first based on random stationary processes,
- second based on the self affine processes with multiscale nature,
- third based on the theory of chaotic dynamics.

In reality the multiperiodic components are often mixed with random noise.

Before choosing the approach, some preliminary analysis is needed mainly to test the stationarity and linearity. This is important as some kind of stochastic (self affine) processes with power-law shape of their spectrum may erroneously be classified as chaotic processes on the basis of some properties of their non-linear characteristics, e.g., correlation dimension and Kolmogorov entropy. In this sense, the tests for stationarity and linearity may be regarded as a necessary preprocessing in order to choose an appropriate approach for further analysis. Prior to selecting any method for data analysis, some simple tests are useful to apply on the series $R_{(i)}$. The first one may be to observe the $R_{(i)}$ distribution e.g. via histogram as simple estimator of probability density function (pdf) or by using kernel density estimator (Meloun & Militký, 2011). The histogram of series $R_{(i)}$ corresponding to the raw SHV trace of twill weave fabric (shown in the fig. 4) is shown in fig. 14.
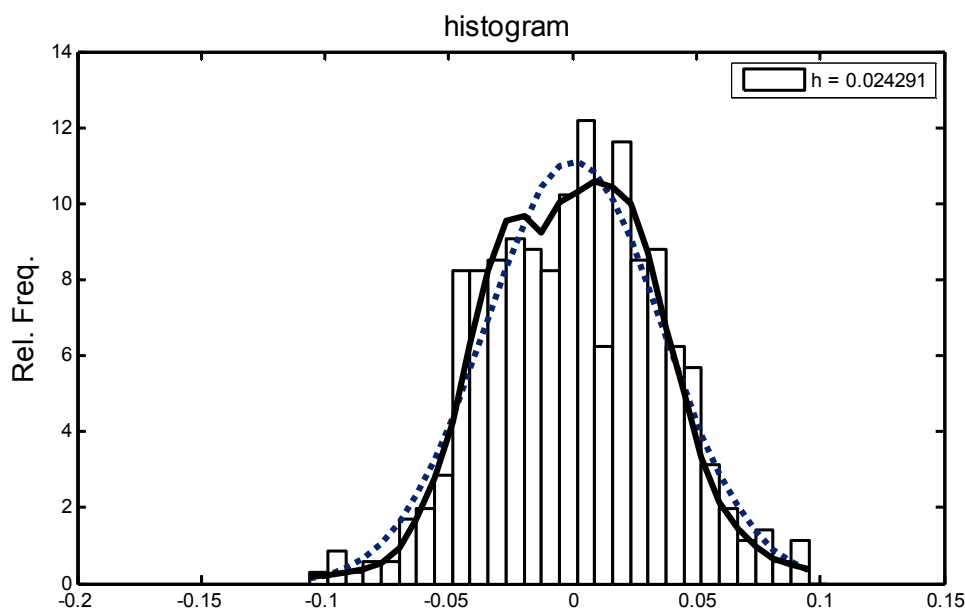

Fig. 14. Histogram and pdfs of raw SHV for twill fabric

In this figure, the solid line corresponds to the Gaussian pdf with parameters: mean = 0.000524 and standard deviation = 0.0358. The dotted line is nonparametric kernel density estimator wit optimal bandwidth h= 0.0243. The bimodality pattern is clearly visible.

In most of the methods for data processing based on stochastic models, normal distribution is assumed. If the distribution is proved to be non-normal (according to some test or inspection), there are three possibilities:

1. the process is linear but non-gaussian;
2. the process has linear dynamics, but the observations are as a result of non-linear "static" transformation (e.g. square root of the current values)
3. the process has non-linear dynamics.

It is suitable to construct the histograms for the four quarters of data separately and inspect non-normality or asymmetry of distribution. The statistical characteristics (mean and variances) of these sub series can support wide sense stationarity assumption (when their values are statistically indistinguishable).

The simple nonparametric test of stationarity uses the reverse arrangement evaluation. Test is based on the computation of times that $R_{(i)} > R_{(j)}$ with i < j for all i. If the sequence of $R_{(i)}$ are independent identically distributed (i.i.d) random variables, the number of reverse arrangements *NR* is random variable with mean *E(NR) = N(N-1)/4* and variance *D(NR) = N(2N+5) (N+1)/72*. If observed number *NR* is significantly different from *E(NR)*, the non-stationarity (trend) is indicated. For rough SHV from fig. 4 reversation test statistic NT = 2.328 and upper limit for P=95%, is 1.96 only. The stationarity is therefore not acceptable.

The alternative "run test" can detect a monotonic trend in a series $R_{(i)}$ i = *1..N*. A "run" is defined as a sequence of identical observations that is followed or preceded by a different observation or no observation at all. First the median *med (R)* of the observations $R_{(i)}$ is evaluated and the new series z(i) is derived from $R_{(i)}$ as

$$z\ (i) = 0\ \text{if } R_{(i)} < med\ (R)$$

$$z\ (i) = 1\ \text{if } R_{(i)} \geq med\ (R)$$

Then the member of runs in z(i) is computed. If $R_{(i)}$ is stationary random process, the number of runs *NT* is a random variable with mean *E(NT) = N/2 + 1* and variance *D(NT) = (N(N – 2)) /(4(N-1))*. As observed number of runs *NT* is significantly different from *E(NT)*. It indicates nonstationarity because of the possible trend. For rough SHV from fig. 4, *NR*= 18.14 and upper limit for P=95% is 1.96 only. The stationarity is here not acceptable.

Very simple check of presence of first order autocorrelation is creation of zero order variability diagram which is plot of $R_{(i+1)}$ on $R_{(i)}$. In the case of independence the random cloud of points appears on this graph. Autocorrelation of first order is indicated by linear trend.

For characterization of independence hypothesis against periodicity alternative the cumulative periodogram can be constructed. Cumulative periodogram is unbiased estimate of the integrated spectrum

$$CU(f_i) = \frac{\sum_{j=1}^{i} I(f_j)}{N\ s^2} \tag{4}$$

The function *C(fi)* is called the normalized cumulative periodogram (construction of *I(fi)* is described in par. 7). For white noise series (i.i.d. normally distributed data), the plot of *C(fi)* against *fi* would be scattered about a straight line joining the points (0, 0) and (0.5, 1). Periodicities would tend to produce a series of neighboring values of *I(fi)* which were large. The result of periodicities therefore bumps on the expected line. The limit lines for 95% confidence interval of *C(fi)* are drawn at distances $\pm 1.36 / \sqrt{(N-2)/2}$. For rough SHV from fig. 4 cumulative periodogram is shown in fig. 15.

6. Aggregation principle

In the unevenness analysis, it is common to aggregate raw data. This is equivalent to cutting the material to pieces and measurement of variability between pieces only. In the case of
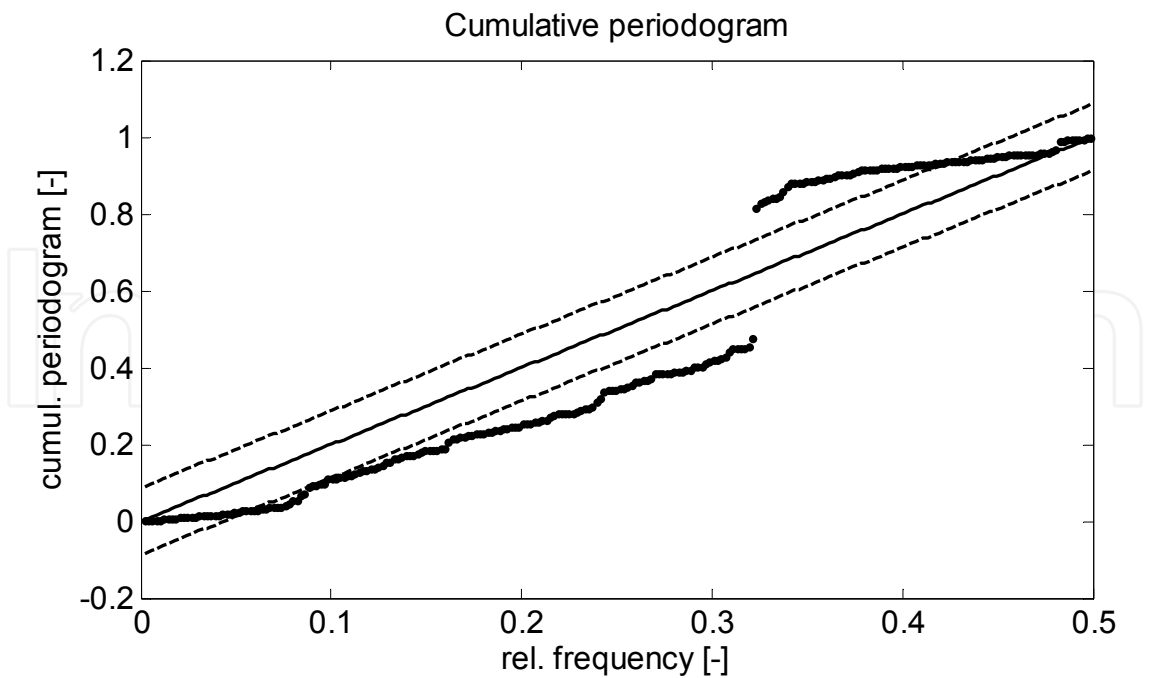
Fig. 15. Cumulative periodogram of raw SHV for twill fabric
It is visible that the raw SHV is approximately periodic.

roughness aggregation is tool for smoothing of roughness profiles and avoiding local (small scale) roughness. The principle of aggregation is joining of original data $R_{(i)}$ into non overlapping blocks or application of window of length L. By using of aggregation the resolution is decreased and roughness profile is created without local roughness variation. By averaging of original data $R_i = R_{(i)}$ in non overlapping blocks having L values the aggregated series are constructed. Aggregated series $R^{(L)}(i)$ are created according to relation

$$R^{(L)}(i) = \frac{1}{L}(R(i\,L-L+1)+..+R(i\,L)) \quad L=1,\,2,\,3..$$ (5)

For rough SHV from fig. 4, aggregate series for aggregation length $L=2$ and 10 are shown in fig. 16.

It is known (Beran, 1984; Cox, 1984) that variance of aggregated series $v^{(L)}$ is connected with auto correlation structure of original series

$$v^{(L)} = \frac{v}{L} + \frac{2}{L^2}\sum_{s=1}^{L-1}\sum_{h=1}^{s}c(h)$$ (6)

Here $c(h)$ is autocorrelation function defined as $c(h) = \text{cov}(R(i)*R(i-h))$ and lag $h = L*d_i$. Very important is lag one autocorrelation function for aggregated series

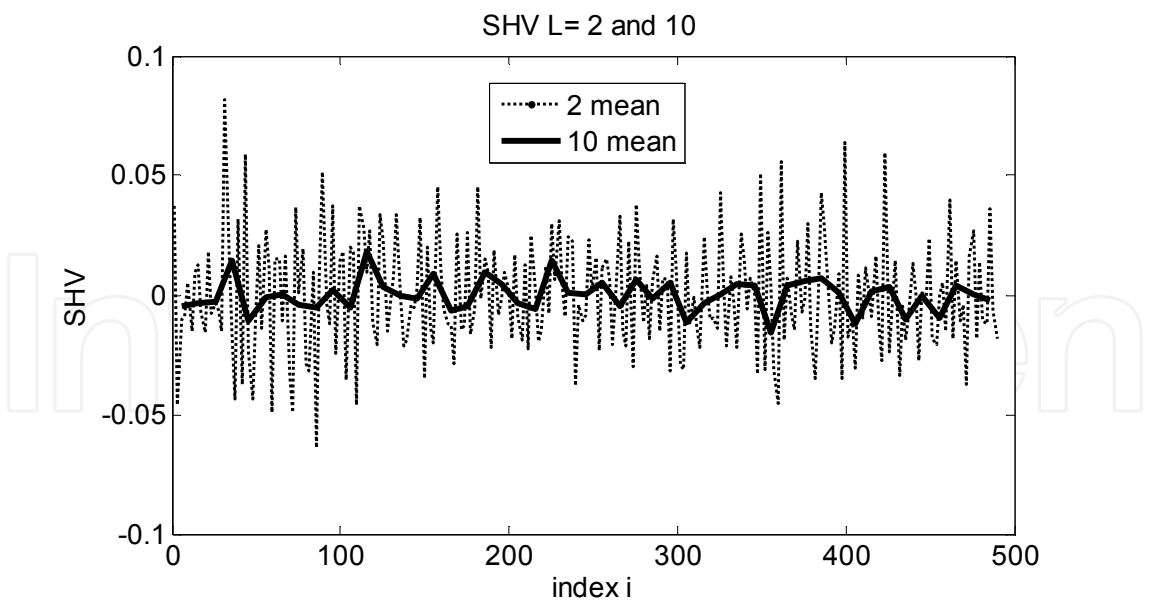$$r^{(L)}(1) = 2\,\frac{v^{(2*L)}}{v^{(L)}} - 1$$ (7)

Fig. 16. Aggregate series (L =2 and 10) for twill fabric

The nature of original random series can be explained by using of characteristics of aggregated series. There are three main groups of series:

1. Series of random independent identically distributed (i.i.d.) variables. For this case are all *c(h) =0*, for lags h = 1,2,.. and data are uncorrelated. This is ideal case for roughness analysis and it is implicitly assumed as valid in computation of basic geometric characteristics.
2. The short-range dependent stationary processes. In this case the sum of all *c(h)*
    h= 1, 2, … is convergent
3. The long-range dependent stationary processes. In this case the sum of all *c(h)*
    h= 1, 2, … is divergent

For short-range dependent stationary processes, the first order autocorrelation $r^{(L)}(1) = 0$ for $L \rightarrow \infty$. The same is valid for autocorrelation of all lags h. The aggregated series $R^{(L)}(i)$ therefore tends to the second order pure noise as $L \rightarrow \infty$. For large L variance $v^{(L)} = v / L$. The autocorrelation structure of aggregated series is decreased until limit of no correlation. Typical model of short-range processes are autoregressive moving average processes of finite order. For the higher *L,* data are approaching to the i.i.d. case.

For long-range dependent processes, variance $L\, v^{(L)} \rightarrow \infty$ as $L \rightarrow \infty$.

Then the autocorrelation structure is not vanishing. For these processes, it is valid that for sufficiently large L

$$c(h) \approx h^{-\beta} \text{ and } v^{(L)} \approx L^{-\beta} \tag{8}$$

where $0 < \beta < 1$ is valid for stationary series. For non-stationary case β can be outside of this interval. For the long-range processes correlation structure is identical for original and aggregate series. For strictly second order self-similar processes,

$$c(h) \approx \frac{v}{2}(1-\beta)\,(2-\beta)\,h^{-\beta} \tag{9}$$

For the higher L the correlation structure remains the same and assumption of i.i.d. cannot be used. Instead of β the so-called Hurst exponent $H = 1 - 0.5 * \beta$ is frequently used. Where H = 0, this denotes a series of extreme irregularity and $H = 1$ denotes a smooth series.

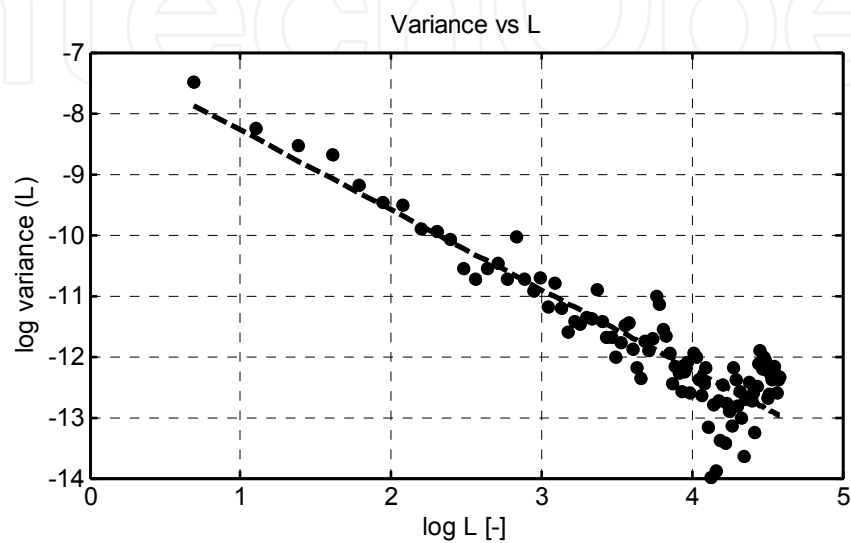For rough SHV from fig. 4 dependence of $log\ v^{(L)}$ on aggregation length L shown in fig. 17.

Fig. 17. Dependence of $log\ v^{(L)}$ on L for twill fabric

It is clear that for higher L this dependence is scattered and corresponding slope is over 1.

The long range dependency is characteristic for self affine processes as well. Self similar processes are characterized by the fractal dimension *FD*. For self-affine processes, the local properties are reflected in the global ones, resulting in the well known relationship *H + FD = 2*. Long-memory dependence, or persistence, is associated with the case *H ∈ (0.5 ,1)* and linked to smooth curves with low fractal dimensions. Rougher curves with higher fractal dimensions occur for antipersistent processes with *H ∈ (0, 0.5)*.

If $1 - c(h) \approx h^{-\alpha}\ for\ \alpha \to 0$, the process has called fractal dimension $FD = 2 - \alpha / 2$. Generally, the *l*-th central moment of aggregated long range dependent series is defined as

$$M_l^{(L)} = \frac{1}{N/L} \sum_{k=1}^{N/L} abs(y^{(L)}(k) - \overline{y})^l \tag{10}$$

The $M_l^{(L)}$ asymptotically behaves like power function $M_l^{(L)} \approx L^{l(H-1)}$. If the series has finite variance and no long-range dependence, then *H = 0.5* and the slope of the fitted line in log-log plot of $M_l^{(L)}$ on L should be – *l/2*. It is assumed that both *N* and *N/L* are large. This ensures that both the length of each block and number of blocks is large. In practice the points at very low and high ends of the plot are not used for fitting least squares line. Indeed, short-range effects can distort the estimates of *H* if the low end of plot is used.

One of the best methods for evaluation of β or H is based on the power spectral density

$$g(\omega) = \frac{1}{2\pi} \int\limits_{h=-\infty}^{\infty} c(h) \ \exp(-i \ h \ \omega) \ d\omega \quad -\pi < \omega < \pi \tag{11}$$

For small frequency range, it is valid that

$$g(\omega) \approx \omega^{-(1-\beta)} \quad \omega \to 0 \tag{12}$$

and for very high frequency range

$$g(\omega) \approx \omega^{-1-\alpha} \quad \omega \to \infty \tag{13}$$

The parameters β and α or are evaluated from empirical linear representation of dependence of the log of power spectral density (PSD) on log frequency in suitable range. The parameter β is often evaluated from empirical representation of the log of power spectral density

$$\log(g(\omega)) = -(1-\beta) \ \log(\omega) + a_0 + a_1 \ \omega + .. + a_p \ \omega^p \tag{14}$$

For long range processes, it is ideal to have all aj = 0, except a_0.

For rough SHV from fig. 4 dependence of $\log(g(\omega))$ on log frequency is shown in fig. 18.
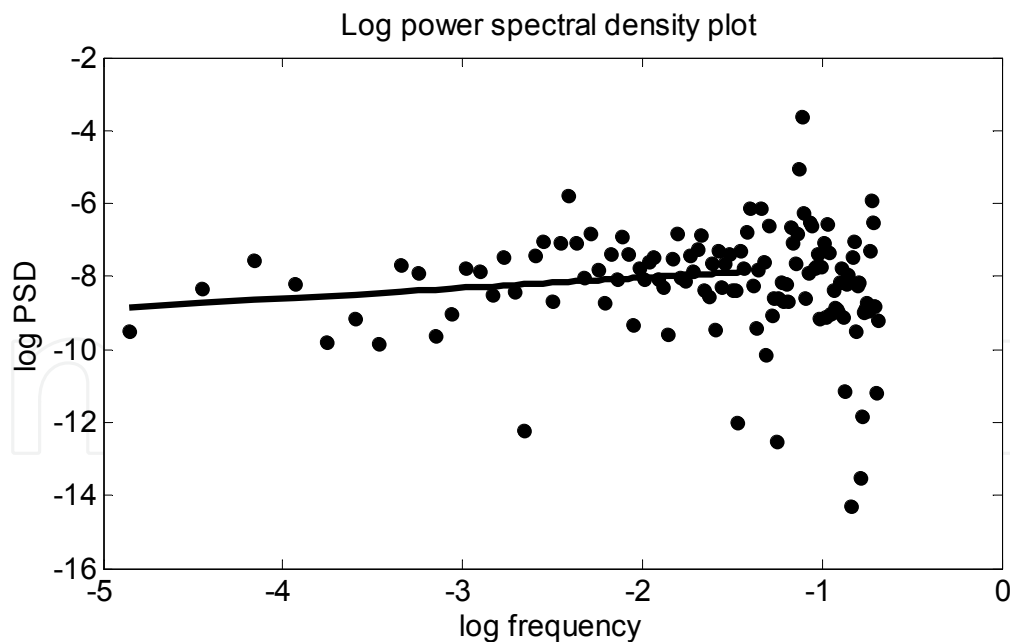
Fig. 18. Dependence of $\log(g(\omega))$ on log frequency for twill fabric

It is visible that the scatter of data is very big. The solid line in fig. 18 is regression line created for low frequency range data set. The slope is equal to - 0. 2831. Corresponding β = 0.7169 and Hurst exponent is 0.6416.

7. Classical roughness characteristics

Because the basic output form RCM is set of "slices" (roughness profiles in the cross direction at selected position in machine direction) it is possible to compute all profile roughness characteristics separately for each slice and show the differences between slices. Another possibility is to use the reconstructed surface roughness plane for evaluation of planar roughness.

There are two reasons for measuring surface roughness. First, is to control manufacture and is to help to ensure that the products perform well. In the textile branch the former is the case of special finishing (e.g. pressing or ironing) but the later is connected with comfort, appearance and hand.

From a general point of view, the rough surface display process which have two basic geometrical features:

- Random aspect: the rough surface can vary considerably in space in a random manner, and subsequently there is no spatial function being able to describe the geometrical form,
- Structural aspect: the variances of roughness are dependent with respect to their spatial positions and their correlation depends on the distance. Especially surface of textile weaves is characterized by nearly repeating patterns and therefore some periodicities are often identified.

The random part of roughness can be suppressed by proper smoothing. In this case the only structural part will be evaluated.

From the individual roughness profiles, it is possible to evaluate a lot of roughness parameters. Classical roughness parameters are based on the set of points $R(d_j)$ $j = 1.. N$ (SHV) defined in the sample length interval L_s. The distances d_j are obviously selected as equidistant and then $R(d_j)$ can be replaced by the variable R_j. For identification of positions in length scale, it is sufficient to know that sampling distance $d_s = d_j - d_{j-1} = L_s/N$ for $j>1$. The standard roughness parameters used frequently in practice are (Anonym, 1997):

i. Mean Absolute Deviation *MAD*. This parameter is equal to the mean absolute difference of surface heights from average value *(R_a)*. For a surface profile this is given by,

$$MAD = \frac{1}{N}\sum_j \left| R_j - \bar{R} \right| \qquad (15)$$

This parameter is often useful for quality control and textiles roughness characterization (called SMD (Kawabata, 1980)). However, it does not distinguish between profiles of different shapes. Its properties are known for the case when $R_j's$ are independent identically distributed (i. i. d.) random variables. For rough SHV from fig. 4, dependence of SMD on aggregation length L is shown in fig. 19.

ii. Standard Deviation (Root Mean Square) Value *SD*. This characteristics is given by

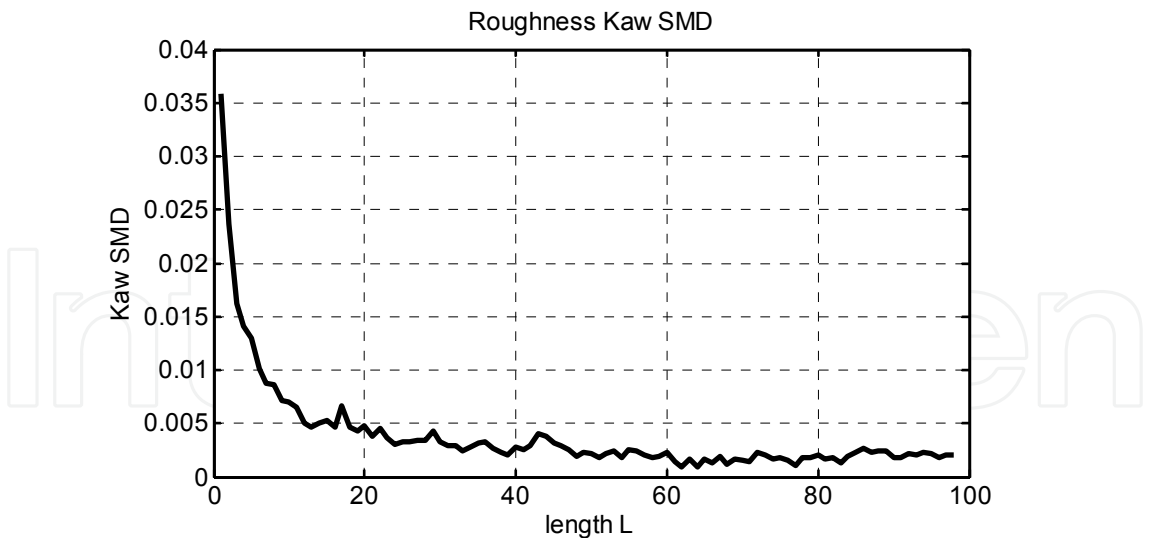$$SD = \sqrt{\frac{1}{N}\sum_j (R_j - \bar{R})^2} \qquad (16)$$

Fig. 19. Dependence of SMD on the aggregation length *L* for twill fabric

The influence of teeth profile parameters am and ym on MAD is shown in the fig. 20.
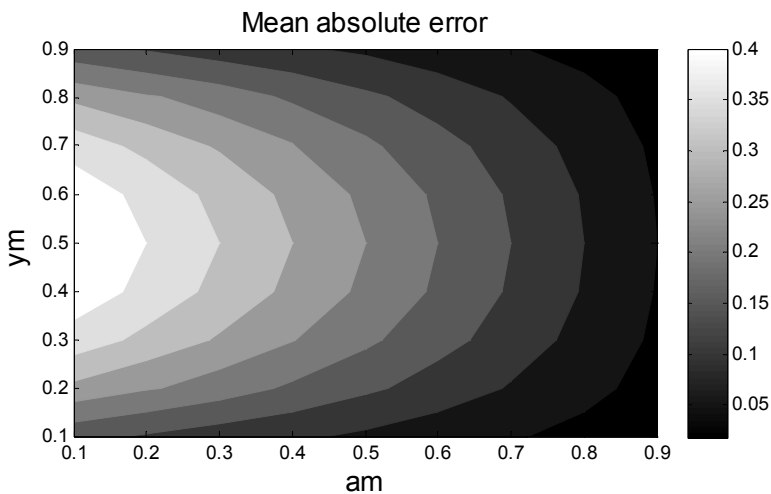

Fig. 20. Influence of am and ym on the MAD

Its properties are known for the case when $R_j's$ are independent identically distributed (i.i.d.) random variables. One advantage of SD over MAD is that for normally distributed data, it can be simple to derive confidence interval and to realize statistical tests. SD is always higher than MAD and for normal data *SD = 1.25 MAD*. It does not distinguish between profiles of different shapes as well. The parameter *SD* is less suitable than MAD for monitoring certain surfaces having large deviations (corresponding distribution has heavy tail).
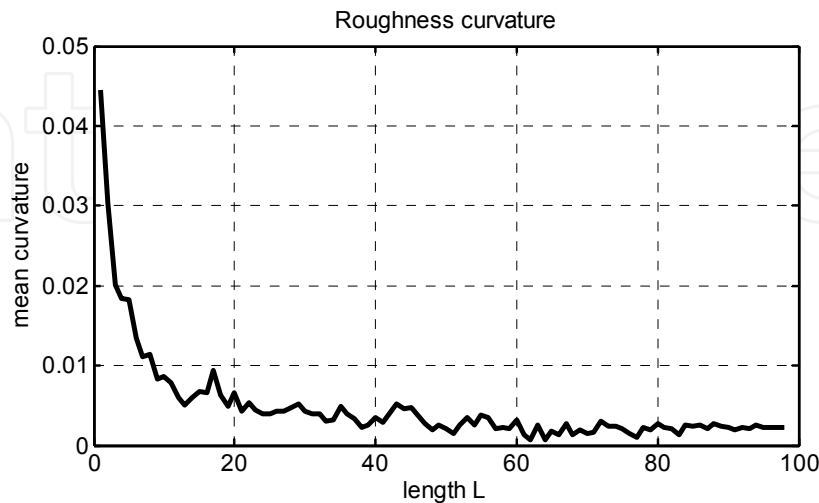
The influence of teeth profile parameters *am* and *ym* on the square of SD (i.e. variance) is shown in the fig. 21.

It is visible that the MAD and SD have similar dependence on the tooth parameters *am* and *ym*. SD is always higher than MAD and for normal data SD = 1.25 MAD. It does not distinguish between profiles of different shapes as well. The parameter SD is less suitable

than MAD for monitoring certain surfaces having large deviations (corresponding distribution has heavy tail).
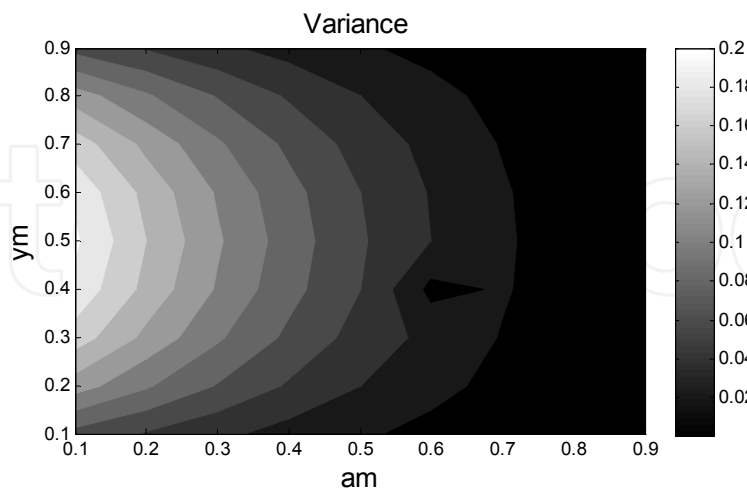
Fig. 21. Influence of *am* and *ym* on the variance (square of SD)

iii. The Standard Deviation of Profile Curvature *PC*. This quantity called often as waviness is defined by the relation

$$PC = \sqrt{\frac{1}{N} \sum_j \left(\frac{d^2 R(x)}{dx^2} \right)_j^2} \qquad (17)$$

The curvature is characteristics of a profile shape. The *PS* parameter is useful in tribological applications. The lower the slope, the smaller will be the friction and wear. Also, the reflectance property of a surface increases in the case of small *PC*.

For rough SHV from fig. 4 dependence of PC on aggregation length L is shown in fig. 22.

Fig. 22. Dependence of SMD on aggregation length *L* for twill fabric

The influence of teeth profile parameters *am* and *ym* on the PS are shown in the fig. 23.
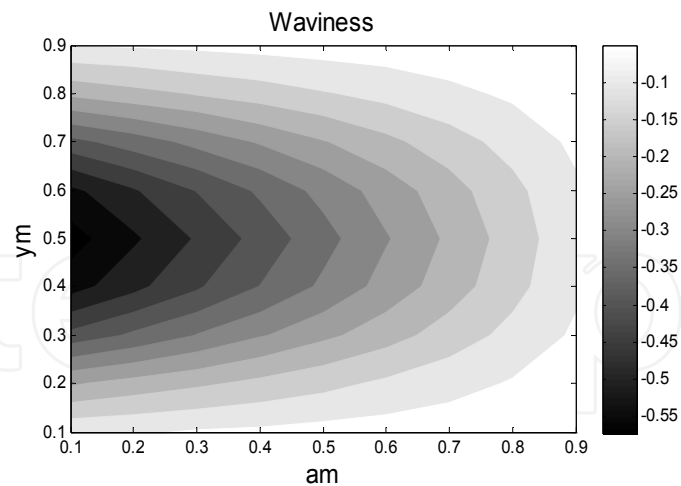
Fig. 23. Influence of *am* and *ym* on the PC

It is visible that the growing of *am* (i.e. decreasing of tooth thickness) leads to the increase of PC. Lowest values of PC are around *ym* equal to the 0.5. This behavior is "inverse" to the behavior of MAD and SD. The PC parameter is useful in tribological applications. The lower the slope the smaller will be the friction and wear. Also, the reflectance property of a surface increases in the case of small PC.

The *MAD* and *PC* characteristics for all slices for cord fabric (see fig. 11) are shown in the fig. 24.

a)   b)
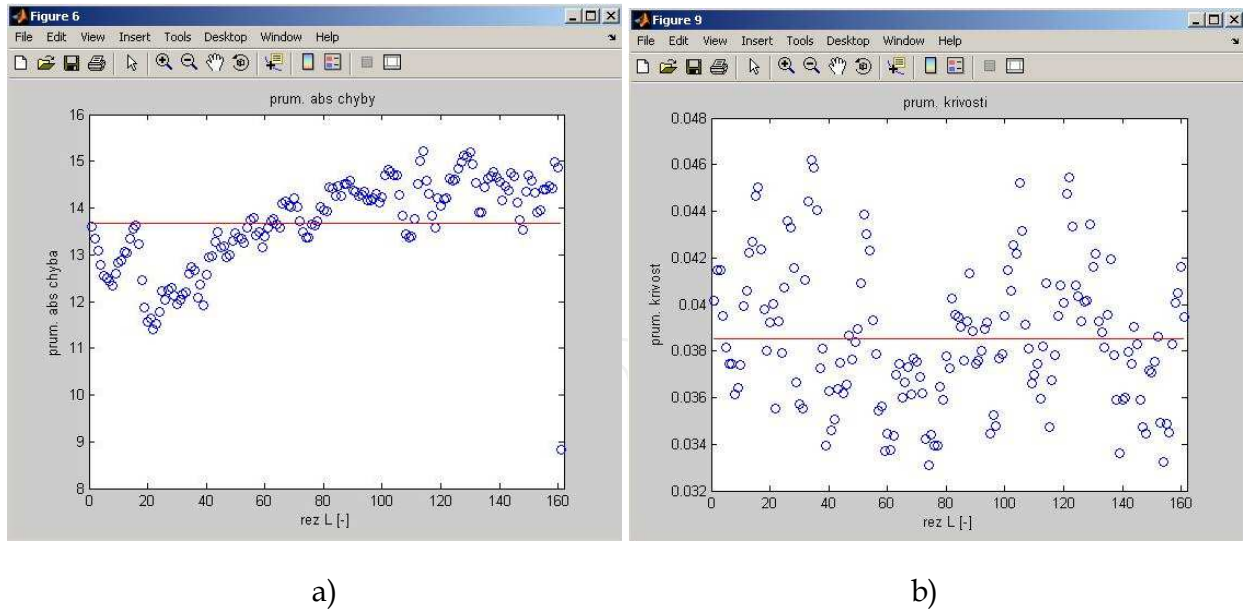
Fig. 24. The a) MAD and b) PC values for all slices of cord fabric (fig. 11)

In the case of MAD, a systematic trend is visible. The variation of PC is nearly random.

For the characterization of hand, it will be probably the best to use waviness *PC*. The characteristics of slope and curvature can be computed for the case of fractal surfaces from power spectral density, autocorrelation function or variogram.

8. Spectral analysis

The primary tool for evaluation of periodicities is expressing of signal $R(d)$ by the Fourier series of sine and cosine wave. It is known that periodic function given by equally spaced values R_i, $i = 0, ..., N - 1$ can be generally expressed in the form of Fourier series at Fourier frequencies $f_j = j/N$, $1 \leq j \leq [N/2]$. If N is odd with $N = 2m + 1$, the Fourier series has form (Quinn & Hannan, 2001)

$$R_i = a_0 + \sum_{k=1}^{m} \left(a_k \, \cos(\omega_k \, i) + b_k \, \sin(\omega_k \, i) \right) \quad i = 0, .. \, N - 1 \tag{18}$$

where $\omega_k = 2 \, \pi \, f_k = 2 \, \pi \, k \, / \, N$ $k = 1, .. \, m$ $k = 1, ..., m$ are angular frequencies. The eqn. (17) is for known frequencies harmonic linear regression model with $2m + 1$ parameters (intercept and $2m$ sinusoids amplitudes at the m Fourier frequencies). The sinusoid with the j-th Fourier frequency completes exactly j cycles in the span of the data. Due to selection of Fourier frequencies all regressors ($sin(.)$ and $cos(.)$ terms) are mutually orthogonal, so that standard least-squares method leads to estimates $a_0 = \bar{R}$ and

$$a_k = \frac{2 \sum\limits_{i=0}^{N-1} R_i \, \cos(\omega_k \, i)}{N} \qquad b_k = \frac{2 \sum\limits_{i=0}^{N-1} R_i \, \sin(\omega_k \, i)}{N} \quad k = 1, .. m \tag{19}$$

Basic statistical characteristic in the frequency domain is power spectral density PSD defined as Fourier transform of covariance function.

The simple estimator of power spectral density is called periodogram. The periodogram of an equally spaced series R_i, $i = 0, ..., N - 1$ is defined by equation

$$I(\omega) = \frac{1}{N} \left(\sum_{i=0}^{N-1} R_i \, \cos(\omega \, i) \right)^2 + \frac{1}{N} \left(\sum_{i=0}^{N-1} R_i \, \sin(\omega \, i) \right)^2 \tag{20}$$

and can be expressed in the alternate form

$$I(\omega_k) = \frac{N}{4} (a_k^2 + b_k^2) \quad k = 1, .. m \tag{21}$$

For rough SHV from fig. 4 periodogram is shown in fig. 25.

The periodogram ordinates correspond to analysis of variance decomposition into m orthogonal terms with 2 degrees of freedom each because,

$$\sum_{k=1}^{m} I(\omega_k) = 0.5 \sum_{i=0}^{N-1} \left(R_i - \bar{R} \right)^2 \tag{22}$$

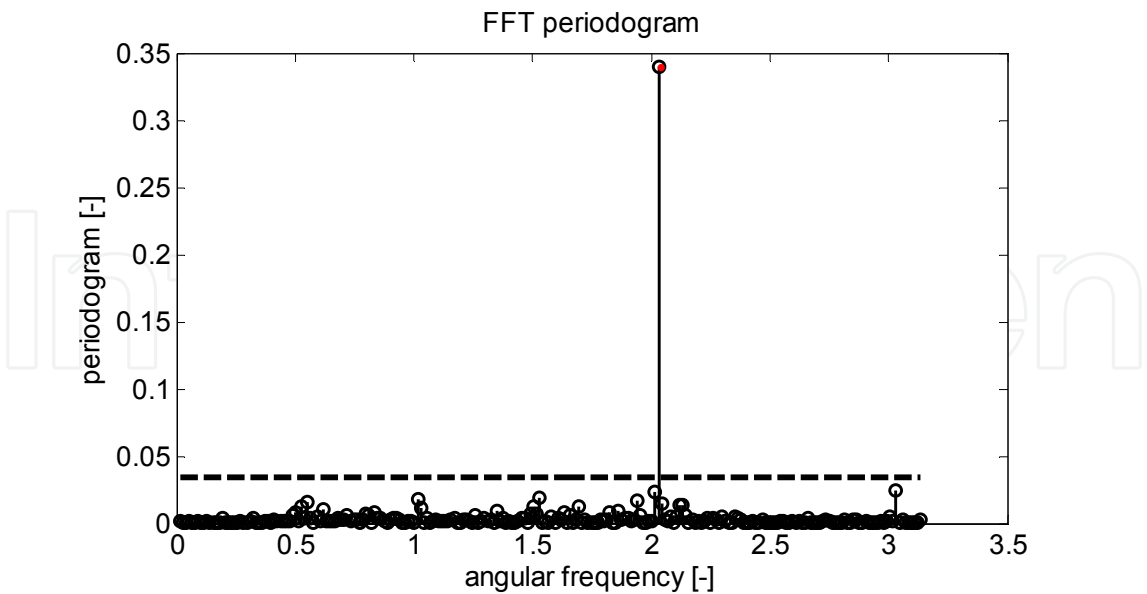The normalized periodogram with ordinates

FFT periodogram

Fig. 25. Periodogram for twill fabric

$$I(\omega_k) / \sum_k I(\omega_k) = A_k / \sum_i (R_i - \bar{R})^2 \qquad (23)$$

is then simply interpretable. The *k-th* ordinate gives the proportion of the total variation due to sinusoidal oscillation at the *k-th* Fourier frequency, and thus is a partial correlation coefficient R^2. The so called scree plot is in fact dependence of relative contribution to the total variance from individual Fourier frequencies arranged according to their importance. For rough SHV from fig. 4, scree plot is shown in fig. 26.
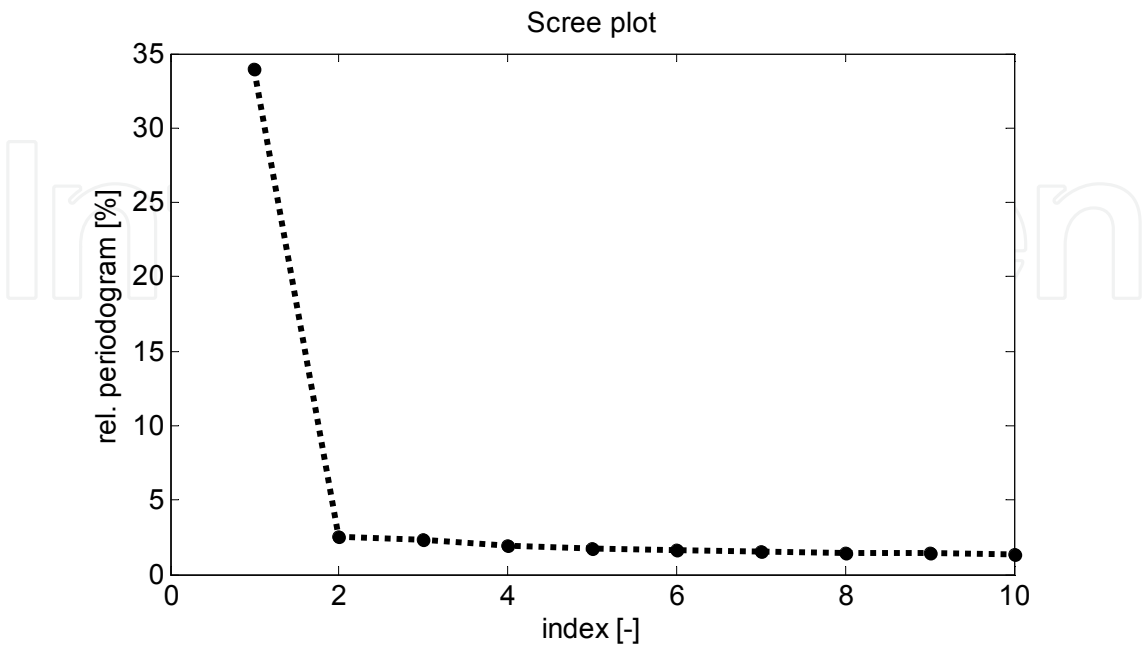
Scree plot

Fig. 26. Scree plot for twill fabric

The well-known trigonometric identity *cos (t- s) = (cos t)(cos s) + (sin t)(sin s)* allows to write each paired sinusoid term as

$$a_k \cos(\omega_k t) + b_k \sin(\omega_k t) = A_k \cos(\omega_k t - \phi_k) \qquad (24)$$

with $A_k = \sqrt{a_k^2 + b_k^2}$ and $\tan(\phi_k) = b_k / a_k$. Coefficients A_k creates amplitude spectrum and coefficients ϕ_k creates phase spectrum.

The influence of teeth profile parameters *am* and *ym* on the amplitude A_1 of most important Fourier term are shown on the fig. 27.
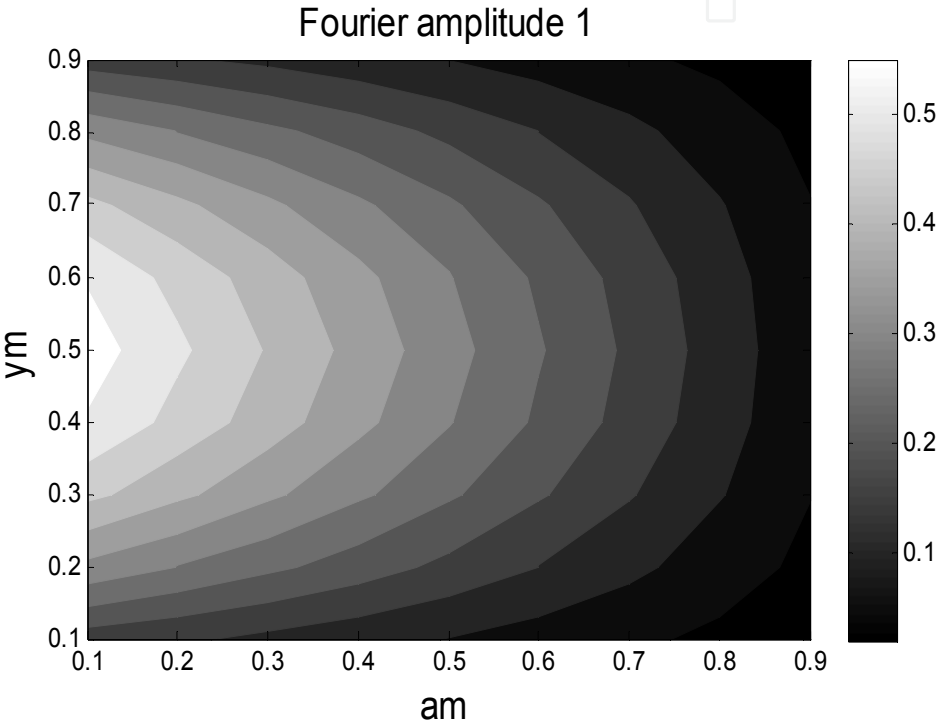
Fig. 27. Influence of *am* and *ym* on the A_1

It is visible that the growing of *am* (i.e. decreasing of tooth thickness) leads to the decrease of the amplitude A_1. Highest values of the amplitude A_1 are around *ym* equal to the 0.5 (similar behaviour as in the case of MAD). The influence of teeth profile parameters *am* and *ym* on the phase ϕ_1 of most important Fourier term are shown on the fig. 28.

It is visible that the growing of *am* (i.e. decreasing of tooth thickness) have the small influence on the phase ϕ_1. The influence of *ym* on the phase ϕ_1 is more important with minimum at *ym* = 0.5.

The periodogram is unbiased only in case of Gaussian noise. The variance of periodogram does not decrease with increasing *N* and has the form

$$D(I(\omega)) \approx I^2(\omega) \left[1 + \left(\frac{\sin(\omega N)}{N \sin(\omega)} \right)^2 \right] \qquad (25)$$

In some cases, it is useful to express Fourier series in the complex exponential form (Quinn & Hannan, 2001).

$$R_i = \sum_{k=1}^{m} \left(C_k \ \exp(\omega_k \ i \ j) \right) \ i = 0, .. \ N - 1 \qquad (26)$$

where j is imaginary unit and complex coefficients C_k have real and imaginary part $C_k = \text{Re}_k + j\text{Im}_k$. The values C_k creates the complex discrete spectrum.
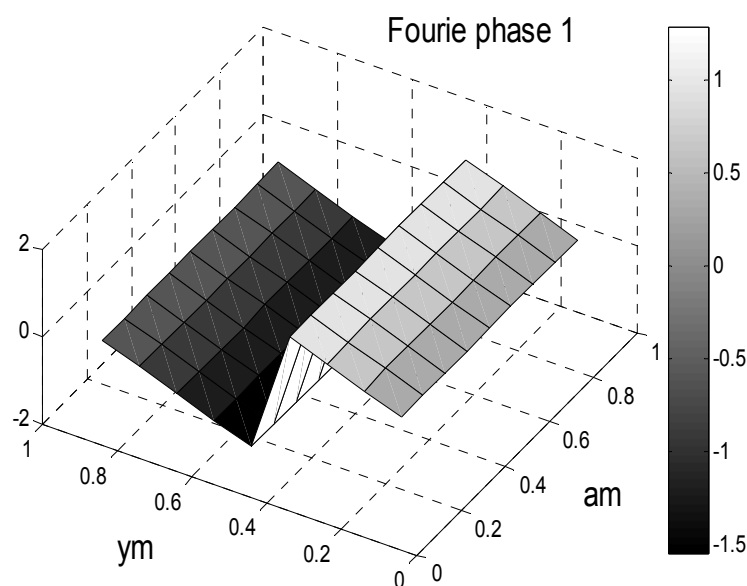

Fig. 28. Influence of *am* and *ym* on the ϕ_1

For discrete data the Fast Fourier Transform (FFT) leads to transformed complex vector *DRF*. The vector *DRF* can be decomposed to the high and low frequency component. After back transformation into original, the SHV part corresponding to noise (high frequencies) and to waviness (low frequencies) can be separated.

For rough SHV from fig. 4 SHV component is corresponding to waviness in fig. 29 and SHV component corresponding to noise is in fig. 30. The number of high frequency components equal to 20 was selected.

Some other techniques for separation of roughness, waviness and form are based on smoothing or digital filtering (Raja et. al, 2002). The smoothing by neural network can be used as well. For estimation of smoothing degree, the minimization of the mean error of prediction is usually applied (Meloun & Militký, 2011).
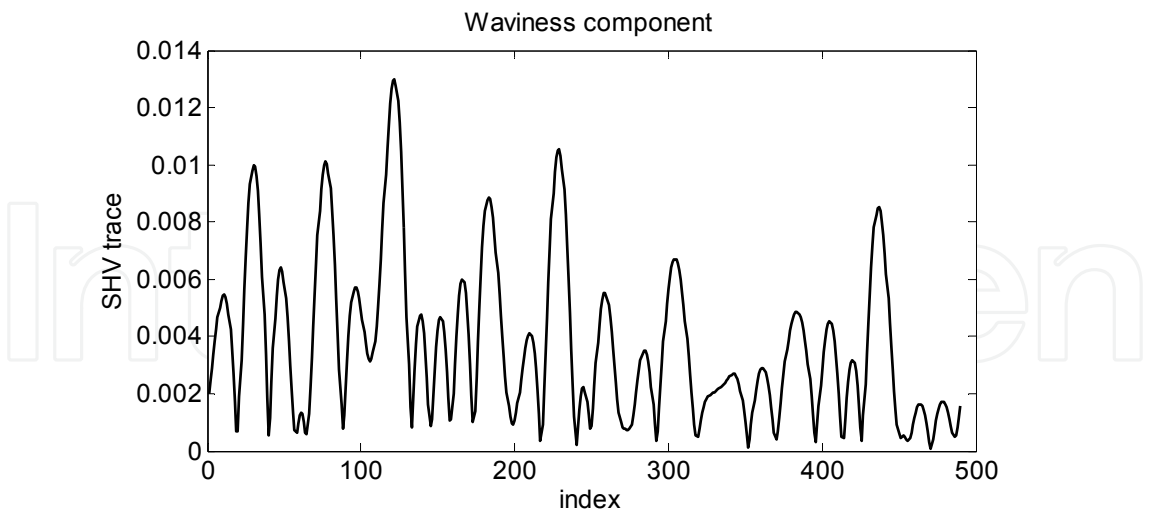
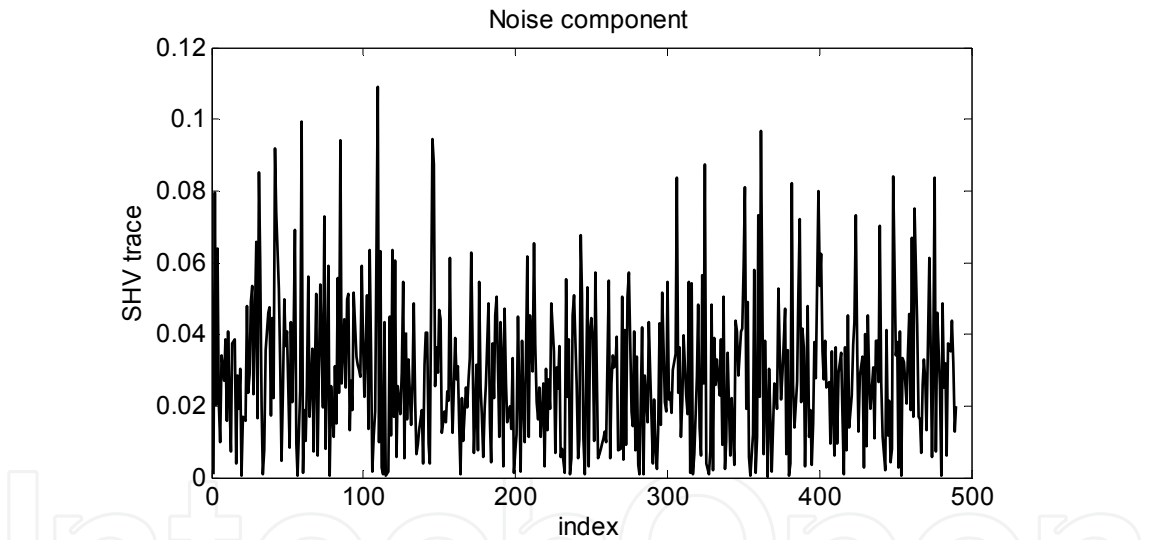Fig. 29. SHV component corresponding to waviness for twill fabric

Fig. 30. SHV component corresponding to noise for twill fabric

Vector *DRF* may be used for creation of power spectral density (PSD)

$$g(\omega) = DRF \; conj(DRF) \,/\, T^2 = abs(DRF)^2 \,/\, T^2 \tag{27}$$

where conj(.) denotes conjugate vector. The $g(T)$ is estimator of spectral density function and contains values corresponding to contribution of each frequency to the total variance of *R*.

The periodogram and power spectral density are primary tool for evaluation of periodicities. Frequency of global maximum on the $I(\omega)$ or $g(\omega)$ graphs is corresponding to the length of repeated pattern and height corresponds to the nonuniformity of this pattern.

Spectral density function is therefore generally useful for evaluation of hidden periodicities. The statistical geometry of an isotropic random Gaussian surface could be expressed in the terms of the moment of power spectral function called spectral moments (Zhang & Gopalakrishnan, 1996).

$$m_k = \int_{\omega_H}^{\omega_L} \omega^k g(\omega) d\omega \tag{28}$$

The m_o is equal to the variance oh heights and m_2 is equal to the variance of slopes between bound frequencies. The frequencies ω_H and ω_L are high and low frequency bounds of integration of the spectrogram. These frequency bound can be converted to the wavelength limits. The long wavelength limit is $l_H = 2\pi / \omega_H$ and the short wavelength limit is $l_L = 2\pi / \omega_L$. For rough SHV from fig. 4, the selected spectral moments have the following values:

- zero moment = 0.0006234.
- first moment = 0.2755.
- second moment = 0.0865.
- fourth moment = 6.387e-006.

Corresponding spectral statistical characteristics are:

- spectral variance = 0.010637.
- spectral skewness = -0.0006368.
- spectral kurtoisis = 0.000342.

The roughness Rq = SD (standard deviation) is simply $Rq = \sqrt{m_0}$ and the density of summits is defined as

$$DS = \frac{m_4}{m_2 \; 6 \; \pi \; \sqrt{3}} \tag{29}$$

9. Analysis in spatial domains

A basic statistical feature of *R(d)* is autocorrelation between distances. Autocorrelation depends on the lag *h* (i.e. selected distances between places of force evaluation). The main characteristics of autocorrelation is covariance function *C(h)*

$$C(h) = \text{cov}(R(d), R(d+h)) = E((R(d) - E(R(d)) \; (R(d+h) - E(R(d)))) \tag{30}$$

and autocorrelation function ACF(h) defined as normalized version of C(h).

$$ACF(h) = \frac{\text{cov}(R(0) \; R(h))}{v} = \frac{c(h)}{c(0)} \tag{31}$$

ACF is one of main characteristics for detection of short and long-range dependencies in dynamic series. It could be used for preliminary inspection of data.

The computation of sample autocorrelation directly from definition for large data is tedious. The spectral density is the Fourier transform of covariance function $C(h)$

$$g(\omega) = \frac{1}{2\pi} \int_0^\infty C(t) \, \exp(-i \, \omega \, t) dt \tag{32}$$

The ACF is inverse Fourier transform of spectral density.

$$ACF(h) = \int_0^\infty S(\omega) \, \exp(i \, \omega \, h) d\omega \tag{33}$$

These relations show that characteristics in the space and frequency domain are interchangeable.

For rough SHV from fig. 4 is *ACF* till lag 320 component in the fig. 31.
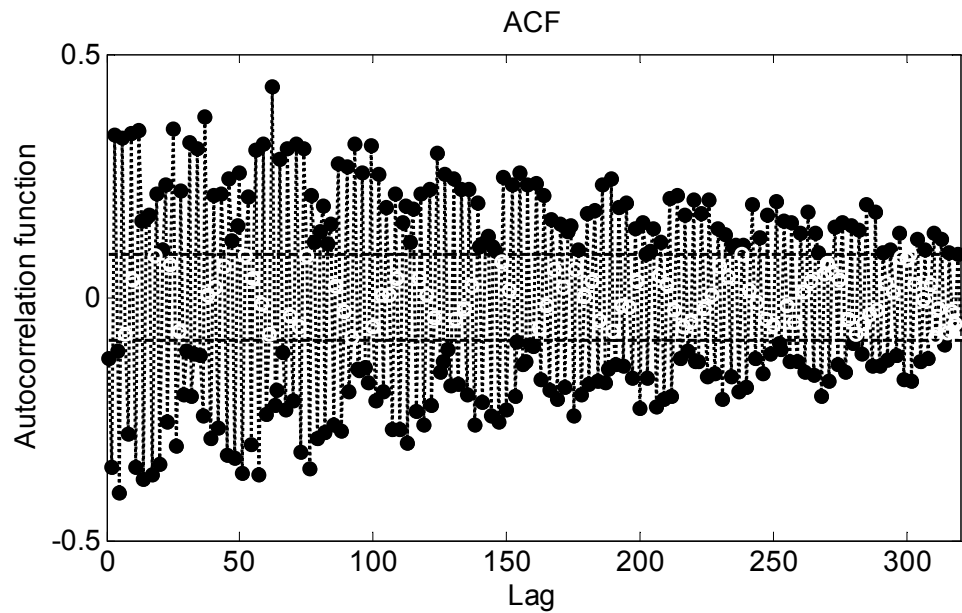
Fig. 31. ACF for twill fabric

The dashed lines in fig. 31 are the approximate 95% confidence limits of the autocorrelation function of an IID process of the same length. Sample autocorrelations lying outside the 95% confidence intervals of an IID process are marked by black circles. The slow decrease of ACF for large lags indicates long-range correlation, which may be due to non-stationarity and/or dynamic non-linearity.

In spatial statistics variogram is more frequent (Kulatilake et. al, 1998) which is defined as one half variance of differences $(R(d) - R(d+h))$

$$\Gamma(h) = 0.5 \, D[R(d) - R(d + h)] \tag{34}$$

The variogram is relatively simpler to calculate and assumes a weaker model of statistical stationarity, than the power spectrum. Several estimators have been suggested for the variogram. The traditional estimator is

$$G(h) = \frac{1}{2M(h)} \sum_{j=1}^{M(h)} (R(d_j) - R(d_{j+h}))^2 \tag{35}$$

where $M(h)$ is the number of pairs of observations separated by lag h. Problems of bias in this estimate when the stationarity hypothesis becomes locally invalid have led to the proposal of more robust estimators. It can be summarized that simple statistical characteristics are able to identify the periodicities in data but the reconstruction of "clean" dependence is more complicated.

10. Roughness anisotropy

Above-mentioned roughness characteristics have implicitly assumed that surface roughness is isotropic phenomenon. This assumption can be accepted in the cases when surfaces have the same micro geometric properties no matter what direction they are investigated in. Majority of textiles structures have anisotropic nature. Surface of woven fabric is clearly patterned due to nearly regular arrangements of weft and warp yarns. The special non-random patterns are visible on knitted structures as well. It is well known that anisotropy of mechanical and geometrical properties of textile fabrics are caused by the pattern and non-isotropic arrangement of fibrous mass. Periodic fluctuations of surface heights can be spatially dependent due to arrangements of yarns. Non-periodic complexity spatial dependence is subtler. The roughness characteristics computed from SHV trace are therefore dependent on the direction of measurements i.e. angle of transect line according to fabric cross direction (perpendicular to machine direction). In KES system, it is possible anisotropy treated by averaging of roughness parameters in weft and warp directions only. This approach is generally over simplified and can lead to under or over estimation of surface roughness.

For anisotropic surfaces the so called surface spectral moments $m_{p,q}$ can be used (Longuet-Higgins, 1957)

$$m_{p,q} = \iint \omega_1^{\,p} \, \omega_2^{\,q} \, S(\omega_1, \omega_2) \, d\omega_1 \, d\omega_2 \tag{36}$$

where $S(\omega_1, \omega_2)$ is bivariate power spectral density of surface. Necessary condition for the case of degenerated spectrum (one dimensional) is

$$2(m_{2,0} \, m_{0,2} - m_{1,1}^2) = 0 \tag{37}$$

For degeneration to more dimensions, similar conditions can be derived (Longuet-Higgins, 1957). The profile spectral moment $m_r(\theta)$ in the direction θ defined by eqn. (27) is connected with surface moments $m_{p,q}$ by relation

$$m_r(\theta) = m_{r,0} \, \cos^r \theta + \binom{n}{1} m_{r-1,1} \cos^{r-1} \theta \, \sin \theta + .. + m_{0,r} \sin^r \theta \tag{38}$$

The second profile spectral moment $m_2(\theta)$, which is equal to the variance of profile slope PS^2, is function of three surface moments $m_{2,0}$, $m_{1,1}$ and $m_{0,2}$ only. This dependence has the simple form derived directly from eqn. (36).

$$m_2(\theta) = m_{2,0}\ \cos^2\theta + 2\ m_{1,1}\ \cos\theta\ \sin\theta + m_{0,2}\ \sin^2\theta \tag{39}$$

The surface moments play central role in description of surfaces topography. The parameters $m_{2,0}$ and $m_{0,2}$, which are the 2nd surface spectral moments, denote the variance of slope in two vertical directions along cross direction and machine direction. The parameter $m_{1,1}$ represents the association-variance of slope in these two directions. These parameters are generally dependent of the selected coordinate system. From the known values of $m_2(\theta_i)$ for selected set of directions θ_i i = 1,..n it is possible to estimate the surface moments $m_{2,0}$, $m_{1,1}$ and $m_{0,2}$ by using of linear regression. The maxima and minima of eqn. (37) are

$$(m_{2\max}, m_{2\min}) = 0,5 * [(m_{2,0} + m_{0,2}) \pm \sqrt{\{(m_{2,0} - m_{0,2})^2 + 4m_{1,1}^2\}}] \tag{40}$$

These occur in the angle θ_p called principal direction given by relation

$$\tan\ \theta_p = \frac{2m_{1,1}}{m_{2,0} - m_{0,2}} \tag{41}$$

As one measure of anisotropy the so-called long-crestedness $1/g$ has been proposed (Longuet-Higgins, 1957), where

$$g = \sqrt{\frac{m_{2\min}}{m_{2\max}}} \tag{42}$$

For an isotropic surface is g = 1 and for degenerated one-dimensional spectrum g = 0. The better criterion of anisotropy has been proposed in the form (Thomas et. al, 1999)

$$AN = 1 - \frac{2 * \sqrt{m_{2,0} * m_{0,2} - m_{1,1}^2}}{m_{2,0} + m_{0,2}} \tag{43}$$

For AN = 0 surface perfectly is isotropic and for AN = 1 surface is anisotropic. Lower AN characteristic indicates low degree of anisotropy.

For investigation of surface roughness anisotropy the twill fabric (see fig. 3) and Krull fabric were selected. The $R(d)$ traces have been obtained by means of KES apparatus in the following directions: θ_i = 0º (weft direction), 30º, 45º, 60º and 90º (warp direction). The Kawabata SMD of individual profiles of twill fabric at chosen directions θ_i is plotted as polar graph in fig. 32 and for Krull fabric in fig. 33.

The surface moments $m_{2,0}$, $m_{0,2}$ and $m_{1,1}$ were computed from eqn. (37) by using of linear least squares regression. Estimated surface moments and AN anisotropy measure are given in the table 1.

The proposed technique is capable to estimate roughness characteristics of anisotropic surfaces typical for textile structures. Beside the anisotropy measure AN the direction θ_p and values of $m_{2\max}$ will be probably necessary for deeper description of textiles surface roughness.
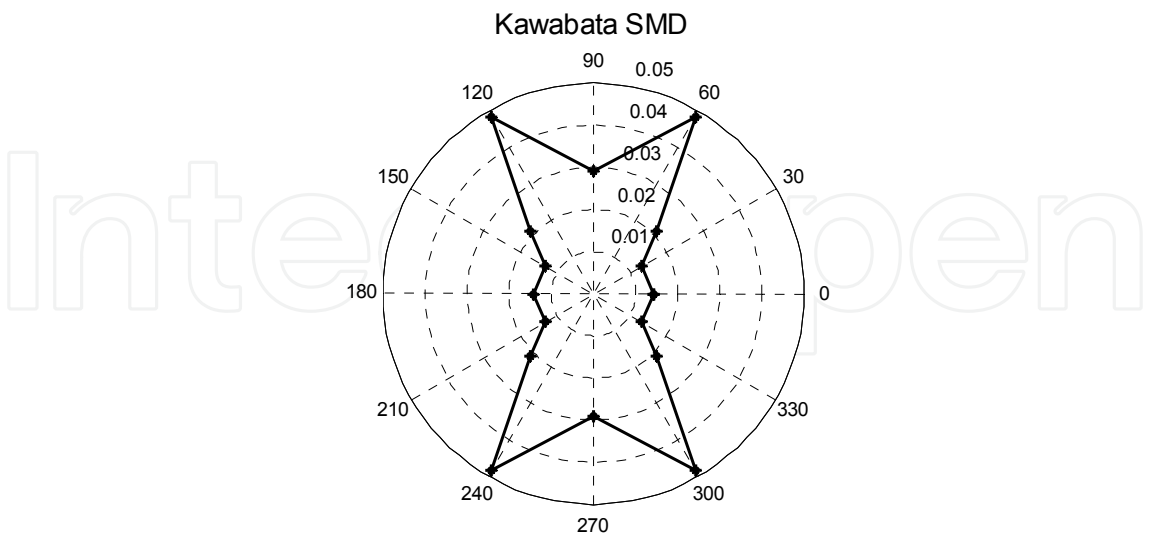
Fig. 32. Kawabata SMD of individual profiles at chosen directions θ_i for twill fabric
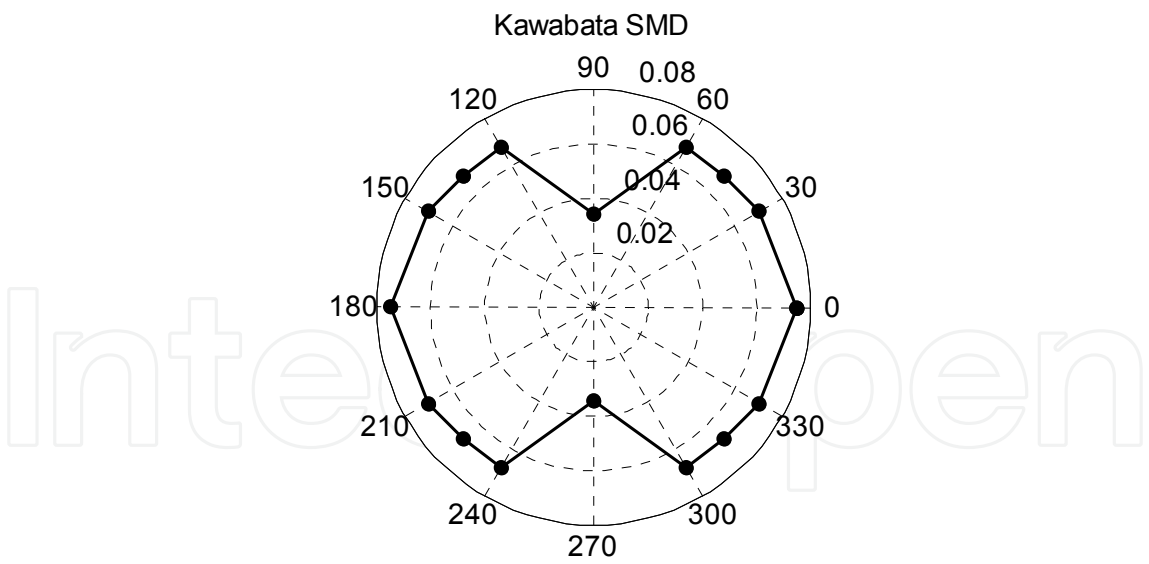

Fig. 33. Kawabata SMD of individual profiles at chosen directions θ_i for Krull fabric

The angular dependence of profile slope variance $m_2(\theta)$ and experimental points for twill are shown on the fig. 34 and for Krull are shown in fig. 35.
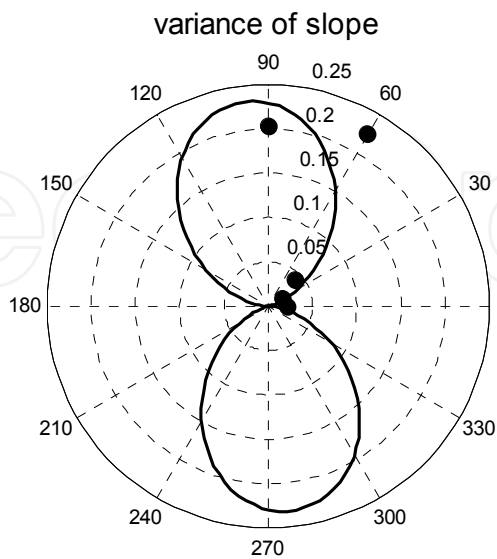
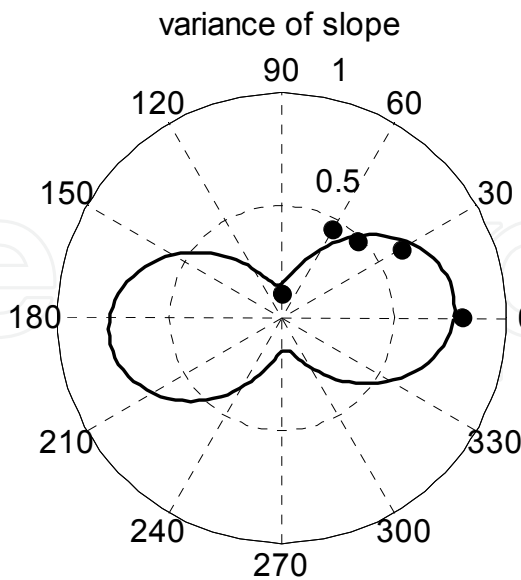Fig. 34. Angular dependence of profile slope variance for twill fabric
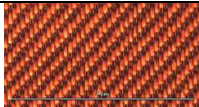

Fig. 35. Angular dependence of profile slope variance for Krull fabric

Pattern	Weave	$m_{2,0}$	$m_{1,1}$	$m_{0,2}$	AN-anisotropy
	Twill	0.0020481	-0.0250585	0.229335	1
	Krull, surface loops	0.7671	0.0613	0.1506	0. 728

Table 1. Surface moments and anisotropy of samples

11. Conclusion

There exists a plenty of other roughness characteristics based on standard statistics or analysis of spatial processes which can be used for separation of noise and waviness (macro roughness). For evaluation of suitability of these characteristics it will be necessary to compare results from sets of textile surfaces.

For deeper analysis of SHV traces from KES device the rough signal registration and digitalization by using of LABVIEW system is beneficial.

The analysis of SHV can be more complex. The other classical roughness characteristics and topothesy can be computed as well and many other techniques of fractal dimension calculation can be included. The analysis can be extended to the chaotic models and autoregressive models. With some modifications it will be possible to use these techniques for characterization of the SHV or surface profiles obtained by other techniques.

The contact less measurement of fabric images by using of RCM device is useful for description of relief in individual slices and in the whole fabric plane.

12. Acknowledgements

13. References

Ajayi, J.O. (1992). Fabric smoothness, Friction and handle, *Text. Res. J.* 62, 87-93

Ajayi, J.O. (1994). An attachment to the constant rate of elongation tester for estimating surface irregularity of fabric, *Text. Res. J.*, 64, 475-476

Anonym, (1997). *ISO 4287: Geometrical product specification, GPS-surface texture, profile method - terms, definitions, and surface texture parameters*, Beuth Verlag, Berlin

Beran, J. (1984).*Statistics for Long -Memory Processes*, Chapman and Hall, New York

Cox, D. R. (1984). *Statistics in Apparaisal*, Iowa State University, 55-74

Davies, S. (1999). Fractal analysis of surface roughness by using of spatial data, *J.R. Stat. Soc.*, 61, 3-37

Eke, A. (2000). Physiological time series: distinguishing fractal noises from motions *Eur. J. Physiol.*, 439, 403-415

Greenwood, J. A. A. (1984). Unified Theory of Surface Roughness, *Proc Roy Soc London*, A393, 133-152

Kawabata, S. (1980). *The standardization and analysis of hand evaluation*, Text. Mach. Soc. Japan

Kulatilake, P. H. S. W. (1998). Requirements for accurate quantification of self affine roughness using the variogram method, *Int. J. Solid Structures* 35, 4167 - 4189

Longuet-Higgins, M. S. (1957). Statistical properties of an isotropic random surface *Phil. Trans. R. Soc. London*, A 250, 157-174

Maisel, L. (1971). *Probability, Statistics and Random Processes*, Simon Schuster, New York

Mandelbrot B.B. & Van Ness J.W. (1968), Fractional Brownian motion, fractional noises and applications, *SIAM Review* 10, 442-460

Meloun, M. & Militký, J. (2011). *Statistical data analysis*, Woodhead Publ. New Delhi

Militký J. & Bajzík V.: (2000) Some open problems of hand prediction, *Journal of Fibers and Textiles*, 7, 141-145

Militký, J. & Bajzík, V. (2001). Characterization of textiles surface roughness, *Proceedings 7th International Asian Textile Conference,* Hong Kong Polytechnic, September

Militký, J. & Bajzík, V. (2002). Surface Roughness and Fractal Dimension, *J. Text. Inst.* 92, Part 3, 1-24

Militký, J. & Bajzík, V. (2004). Characterization of protective clothing surface roughness, *Proc. Int. Textile Congress Technical textiles: World market and future prospects,* Tarrasa, October 251-265

Militký, J. (2007). Evaluation of roughness complexity from KES data*, Proc. 5th International Conference Innovation and Modelling of Clothing Engineering Processes – IMCEP 2007,* Moravske Toplice October

Militký, J. & Klička, V. (2007). Nonwovens Uniformity Spatial Characterization , *Journal of Information and Computing Science* 2, No. 2, 85-92

Militký, J. & Mazal, M. (2007). Image analysis method of surface roughness evaluation, Int. J. Clothing Sci. Technol. 19, 186-193

Militký, J. & Bleša, M. (2008). Evaluation of patterned fabric surface roughness, *Indian Journal of Fibre &Textile Research.* 33, 246-252

Quinn, B.G. & Hannan, E. J. (2001). *The Estimation and Tracking of Frequency*, Cambridge University Press

Raja, J. (2002). Recent advances in separation of roughness, waviness and form, *Journal of the International Societies for Precision Engineering and Nanotechnology* 26, 222–235

Sacerdotti, F. (1996). *Surface Topography in Autobody Manufacture – The state of art*, Brunel University, June

Stockbridge, H. C. (1957). The subjective assessment of the roughness of fabrics, *J. Text. Inst. 48*, T26-34,

Thomas, T. R. (1999). Fractal characterization of the anisotropy of rough surfaces *Wear* 232, 41 – 50

Whitehouse, D. J. (2001). Roughness and fractals dimension facts and fiction, *Wear* 249, 345-346

Zhang, C. & Gopalakrishnan, S. (1996). Fractal geometry applied to on line monitoring of surface finish *Int. J. Mach. Tools Manufact.*, 36, 1137-1150

Woven Fabrics

Edited by Prof. Han-Yong Jeon

"Woven Fabrics" is a unique book which covers topics from traditional to advanced fabrics widely used in IT, NT, BT, ET, ST industry fields. In general, woven fabrics are known as the traditional textile fabrics for apparel manufacturing and are used widely in various fabric compositions as intermediate goods that affect human activities. The relative importance of woven fabrics as traditional textile materials is extremely large and currently application fields of woven fabrics as technical textiles are rapidly expanded by utilizing its geometric features and advantages. For example, the book covers analytical approaches to fabric design, micro and nano technology needed to make woven fabrics, as well as the concept for industrial application.

How to reference

In order to correctly reference this scholarly work, feel free to copy and paste the following:

INTECH

open science | open minds